Isocyanate-free Polyurea Synthesis via Ru-Catalyzed Carbene Insertion into the N–H Bonds of Urea

Felix J. de Zwart,[1] Petrus C. M. Laan,[1] Nicole S. van Leeuwen,[1] Ning Yan,[1] Jitte Flapper,[2] Keimpe J. van den Berg,[3] Joost N. H. Reek[1] and Bas de Bruin[1*]

[1]Homogeneous, Supramolecular and Bio-Inspired Catalysis Group, van 't Hoff Institute for Molecular Sciences (HIMS), University of Amsterdam, Science Park 904, 1098 XH Amsterdam, The Netherlands. [2]Akzo Nobel Decorative Coatings B.V., Rijksstraatweg 31, 2171 AJ Sassenheim, The Netherlands. [3]Akzo Nobel Car Refinishes B.V., Rijksstraatweg 31, 2171 AJ Sassenheim, The Netherlands.

KEYWORDS: Polyureas, Catalysts, Monomers, Ruthenium, Carbene.

ABSTRACT: Polyureas have widespread applications due to their unique material properties. Due to the toxicity of isocyanates, sustainable isocyanate-free routes to prepare polyureas is a field of active research. Current routes to isocyanate-free polyureas focus on constructing the urea moiety in the final polymerizing step. In this study we present a new isocyanate-free method to produce polyureas by Ru-catalyzed carbene insertion into the N–H bonds of urea itself in combination with a series of bis-diazo compounds as carbene precursors. The mechanism was investigated by kinetics and DFT studies, revealing the rate determining step to be nucleophilic attack of a Ru-carbene moiety by urea. This study paves the way to use transition-metal catalyzed reactions in alternative routes to polyureas.

1 INTRODUCTION

Polyurea-based elastomers find widespread applications in foams and coatings due to their unique material properties, such as tensile strength and tear resistance.[1] Routes towards isocyanate-free polyureas and polyurethanes which make use of more benign monomers are of interest due to the toxicity of isocyanates and difficulties in handling these reactive and humidity-sensitive reagents.[2,3] The currently available isocyanate-free routes towards polyureas and polyurethanes can be divided into four broad categories, shown in Scheme 1.[4–6] In rearrangement pathways (Scheme 1a) isocyanates are formed in-situ through Curtius (depicted), Hoffman or Lossen rearrangements.[7] In polycondensation, amines are prefunctionalised with either phosgene or another carbonyl source to furnish a blocked isocyanate, which can then react with an amine or alcohol to yield the desired polyurea (Scheme 1b). Ring opening pathways use cyclic carbamates or ureas that are then polymerized through transcarbamoylation under high temperatures (Scheme 1c) and polyaddition pathways use cyclic carbonates as precursors for polyurethanes (Scheme 1d).[8,9] Most of these isocyanate-free routes have their drawbacks, for example in the formation of isocyanates in-situ (Scheme 1a), acyl azides are used as precursor which are also harmful substances. The polycondensation route (Scheme 1b) releases side-products during curing which limits industrial usage, which in the case of ring-opening is limited by the high temperatures required (Scheme 1c). The most promising route currently utilizes amines and carbonates (Scheme 1d) as precursors with low toxicity.[10]

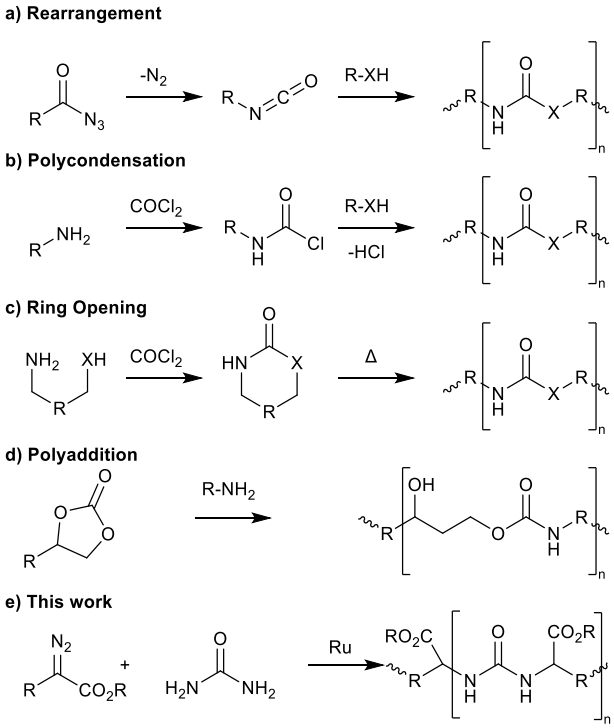

Scheme 1. Synthetic approaches to polyurethanes (X = O) and polyureas (X = NH).

Interestingly, the use of (transition-metal) catalysis to arrive at polyurea and polyurethane structures has not been developed as much. Transition-metal catalyzed polymerizations using diazo compounds provide a powerful alternative synthetic tool to otherwise difficult to access structures.

For example, a variety of diazo compounds can be used as monomers in single-component polymerization, leading to highly functionalized polymers.[11,12] Polyesters and polyethers can be synthesized from their respective alcohols and acids in a co-polymerization reaction with diazo compounds through O–H insertion reactions.[13–15] Using amines as precursor, a recent article by Ihara and coworkers has reported on the synthesis of polyamines through ruthenium catalyzed N–H insertion, a continuation of the research on the synthetic utility of C–N bond formation using diazo compounds.[16–21] Ureas have been used as nucleophiles in transition metal catalysis such as Pd-catalyzed carboaminations and more recently as nitrene precursors in Ru-catalyzed C–H amination.[22–25] Therefore, we envisioned the possibility of using N–H insertions to synthesize polyureas as shown below (Scheme 1e). Whereas in all the known approaches (Scheme 1a–d) the urea moiety is constructed in the final step, this approach differs fundamentally with urea itself operating as a nucleophile to react with a ruthenium centered carbene. Furthermore, with the tunability of diazo precursors a variety of pendant side groups can be attached to influence the material properties of polymers. In this proof-of-concept study we present a new strategy to prepare polyureas by utilizing Ru-catalyzed N–H insertions on urea.

2 RESULTS AND DISCUSSION

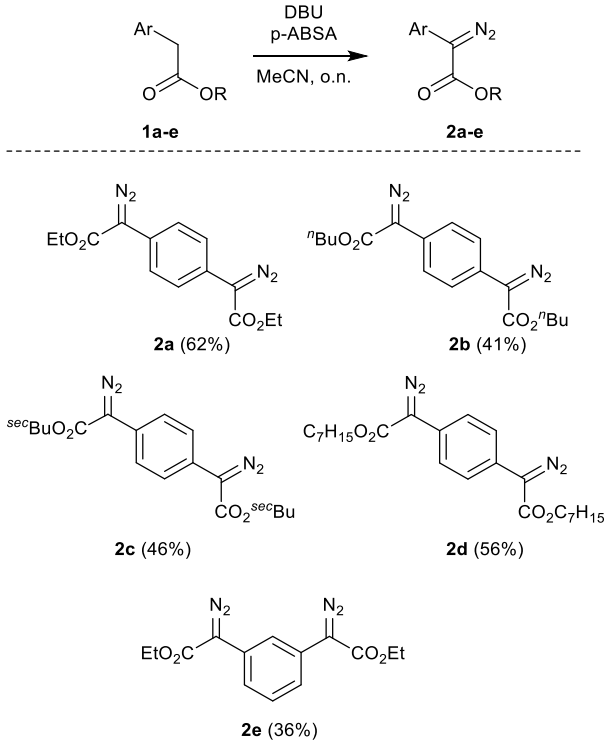

Scheme 2. Synthesis of bis-diazo compounds 2a-e, yield after column chromatography in brackets.

2.1 Bisfunctional Diazo Compound Synthesis. The bisfunctional diazo compound diethyl 1,4-phenylenebis(diazoacetate) **2a** has been described in literature recently, and we decided to expand on the scope of phenylenebis(diazoacetate) compounds by changing the ester substituents.[26] With phenylenediacetic acid as a starting substrate, five different bisfunctional diazo compounds were synthesized in a two-step procedure. The esters are readily synthesized under Dean-Stark conditions in toluene with catalytic amounts of sulfuric acid. The active methylene carbon can be functionalized with a diazo moiety through a Regitz diazo transfer using *p*-acetamidobenzenesulfonyl azide (*p*-ABSA) as a diazo transfer reagent, products **2a-e** were obtained in fair to moderate yields (62-36%) as pure compounds after column chromatography. The diazo compounds were characterized by ^{1}H- and ^{13}C-NMR and HR-MS (see supporting information). Compared to the more often used tosyl azide, *p*-ABSA has the advantage of being less explosive and impact sensitive and is therefore a safer preferred alternative.[27]

Table 1. Polycondensation of 2b with urea.

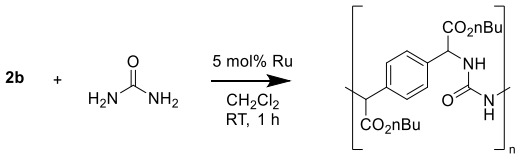

#	Deviations	Yield [a]	M_w (kDa)[b]	$Đ$ [b]
1	None	65%	7.1	1.50
2	10 mol% Ru	94%	6.3	1.61
3	1.1 eq diazo	55%	5.3	1.53
4	1.2 eq diazo	25%	6.1	1.57
5	1.3 eq diazo	0%	-	-
6	0 °C	22%	2.8	1.38
7	25 mL DCM	30%	7.4	1.58
8	1 mL DCM	77%	3.6	1.24

Conditions: urea (100 umol), **2b** (100 umol), dichloro(*p*-cymene)ruthenium(II) dimer (2.5 umol), DCM (2.5 mL), room temperature, 1 hour. [a] Determined by gravimetry after precipitation. [b] M_w/M_n as determined by SEC in DCM.

2.2 Polymerization. The initial exploration of polymerization conditions was started by polycondensation of **2b** with urea in the presence of dichloro(*p*-cymene)ruthenium(II) dimer. This provided a polymeric material, which could be separated from the reaction mixture by precipitation from diethyl ether. The polymer was analyzed by SEC, which revealed a weight-averaged molecular weight (M_w) of 7.1 kD. Increasing the ruthenium catalyst loading led to a higher yield (entry 2, Table 1), while increasing the diazo stoichiometry resulted in a lower yield (entry 3-6, Table 1). These two observations point to a step-growth polymerization process. Decreasing the reaction temperature, or changing the concentration also led to a lower yield or molecular weight (entries 6-8, Table 1). With the optimized polymerization conditions at hand, the scope of the reaction was explored by changing the diazo substituent (Table 2), where diazos **2a-e** were used to synthesize polymers **3a-e**. This provided polymeric materials in good to moderate (65-45%) yields. The slight differences in obtained yields are

presumably a result of the precipitation procedure, as the more soluble *sec*-Butyl substituted polymer **3c** provided the lowest yield. Through size exclusion chromatography (SEC) analysis based on linear polystyrene standards, weight-average molar masses (M_w) and dispersities ($Đ$) of the produced polyureas were estimated to be in the ranges of 3.9-7.1 kD and 1.33-1.59 respectively (Table 2). To corroborate the molecular weight of the polymers, the end group (Figure 2, $H_{b'}/H_b$) signal was integrated against the main chain to obtain the degree of polymerization, which was in agreeance with the degree of polymerization as calculated by SEC (Table 2). We then continued to use polymer **3a** as a starting point for polymer characterization.

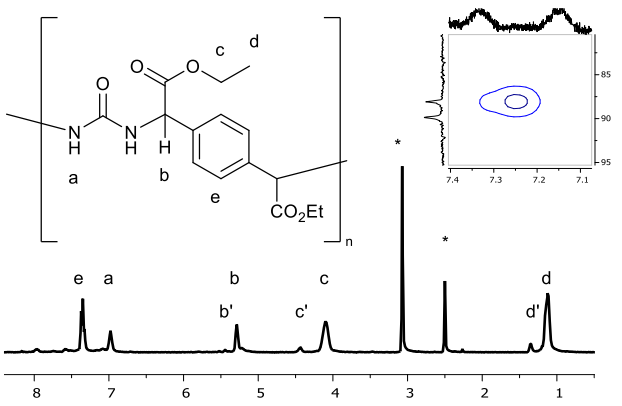

Figure 2. ^{1}H NMR spectra of 2a (*: solvent, primes indicate end-group signals). Inset: ^{1}H-^{15}N HSQC using ^{15}N labeled urea.

2.3 Characterization. The IR spectrum of polyurea **3a** reveals bands located at 3367, 2981, 1732 and 1643 cm^{-1}, which are related to urea N–H, aromatic C–H, ester C=O and urea C=O stretching vibrations, respectively. These bands support the incorporation of both functional groups in the polymer chain and the disappearance of the diazo stretch vibration of the starting material shows full conversion of the bis-diazo compound. The ^{1}H NMR spectrum in DMSO-d_6 at 80 °C (Figure 2) shows characteristic signals for the ethyl chain introduced with co-monomer **2a** at 1.11 and 4.10 ppm (H_d and H_c), and the aromatic protons at 7.35 ppm (H_e). Two new signals at 6.98 and 5.29 ppm are allocated to the urea H_a and benzylic H_b protons. This assignment was confirmed by ^{15}N-labeling of the urea prior to catalysis, providing a ^{15}N-labeled polymer **3a**. The acquired ^{1}H-^{15}N HSQC displays a negative cross-peak, indicative of a secondary amine, between H_a and a doublet in ^{15}N NMR at 89 ppm with a coupling of 91 Hz, supporting the assignment of H_a as the urea N–H proton (Inset Figure 2, see also S40-S41). To confirm the anticipated polymer structure containing alternating urea and phenylene-diester repeating units, ^{13}C NMR analysis was performed, revealing both the ester and urea carbons at 170 and 156 ppm respectively (Figure S39). The ^{13}C-NMR signals belonging to the aromatic ring were located at 137, 130 and 127 ppm. The carbons of the ethyl chain resonate at 60 and 13 ppm, and the benzylic carbon reveals a signal at 56 ppm. The NMR interpretation of polymers **3b**-**3e** is similar to that of **3a** and in accordance with the proposed structure. When using chiral diazo **3c** the benzylic carbon is observed as two signals of equal intensity at 57.3 ppm. This indicates that chiral secondary structures of the resulting polyureas could be accessible when using chiral catalysts capable of enantioselective N–H insertion.

Table 2. Polycondensation of urea with different bisfunctional compounds.

	Yield (%)[a]	M_w (kDa)[b]	DOP (SEC)[b]	DOP (NMR)[c]	$Đ$ [b]	T_g (°C)[d]
3a	56%	4.9	16.2	18.2	1.54	141
3b	65%	7.1	18.6	19.6	1.59	97
3c	45%	4.0	13.1	12.1	1.41	131
3d	57%	4.3	9.6	10.2	1.33	82
3e	54%	3.9	11.0	10.7	1.45	89

Conditions. Urea (100 umol), diazo 2a-e (100 umol), dichloro(p-cymene)ruthenium(II) dimer (2.5 umol), DCM (2.5 mL), room temperature, 1 hour. [a] Determined by gravimetry after precipitation. [b] M_w/M_n, Determined by SEC in DCM. [c] Determined by ^{1}H-NMR in DMSO-d_6 at 80 °C. [d] Determined by DSC.

2.4 Material properties. To investigate the effect of the ester substituent on the material properties, the glass transition temperature (T_g) was measured. Incorporation of soft segments within polyurea segments is known to lead to a decrease in glass transition temperature.[28,29] Indeed, the heptyl substituted polymer **3d** has the lowest T_g, and ethyl substituted diazo **3a** has the highest T_g (Table 2). Furthermore, 1,3-phenylene substituted polymer **3e** is observed to have an intermediate T_g of 89 °C whilst having the same molecular formula as **3a**, showing that main chain connectivity can be used as an effective tool to control the material properties.

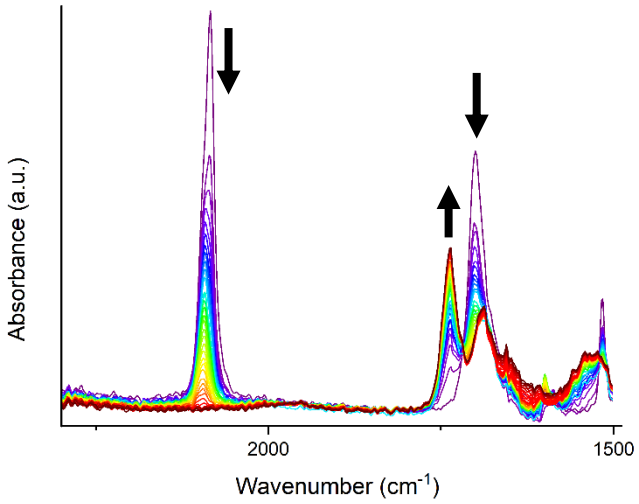

Figure 3. Operando IR monitoring of ruthenium catalyzed polymerization of 2a and urea. One trace corresponds to 15 seconds.

2.5 Kinetics. To obtain more insight in the mechanism of polymerization, the polycondensation of **2a** with urea was followed by operando IR spectroscopy, as shown in Figure 3. A clear decrease in the signal at 2091 cm^{-1}, corresponding to the disappearance of the diazo moiety, of the monomer

was observed. Furthermore, a new signal corresponding to the C=O stretch vibration of the polymer is observed at 1734 cm^{-1}. Using these two signals the conversion and yield over time was monitored to provide insight into the kinetics of this reaction. When using 1,3-substituted diazo **2e**, the conversion decreased linearly over time indicating zeroth order in diazo monomer concentration (Figure S6). On the other hand, with 1,4-substituted diazo **2a** some rate dependence on conversion was observed. To investigate this further with improved time resolution, kinetic experiments were undertaken to derive the rate law for both diazo **2a** and **2e**, by monitoring the gas production of the reaction with a bubble counter.[30] For diazo **2a**, the diazo order dependence in the range of 5–10% catalyst loading was found to not clearly fit to a reaction order (Figure S15–S20). We believe this to be an effect of the *para* substitution on the diazo, causing the electronics of one diazo moiety to be influenced by reactions on the other, thereby complicating the reaction profile. Therefore, the rest of the kinetics were undertaken using *meta*-substituted diazo **2e**, for which the catalytic profile is more clear. As such, for diazo **2e** a first order rate dependence in catalyst concentration was found in the range of 5–10% catalyst loading, excluding any multinuclear pathways (Figure S7–S9). For diazo **2e** a zeroth order dependence of rate upon diazo concentration was found (Figure S10–S12). The low solubility of urea in dichloromethane prevents us from determining the order in urea. The zeroth order kinetic in diazo **2e** suggest that diazo activation is fast, and presumably the follow-up reaction with urea is the rate limiting step. This contrasts with previous work on rhodium X–H insertions, for which carbene formation was shown to be rate limiting.[31] The kinetics in this case should (at least in part) be influenced by the low solubility of urea, which causes the concentration of urea to remain low and constant throughout. Transition metal-catalyzed X–H insertions are generally understood to proceed via a four-step mechanism (Scheme 3a, *vide infra*), consisting of (A) diazo coordination, (B) carbene formation, (C) nucleophilic attack and (D) proton shift.[32,33] Having excluded A and B as rate determining, kinetic isotope effect studies were undertaken using d_4-urea and diazo **2e**. Using the initial rates until 20% conversion the kinetic isotope effect (KIE) for urea was found to be k_H/k_D = 1.31 (Figure S13–S14), corresponding to a secondary kinetic isotope effect.[34] This KIE strongly indicates the rate determining step to be nucleophilic attack, as step C involves rehybridization of the urea nitrogen for which a larger KIE would be expected. This result is different from known copper and rhodium systems,[32] for which fast (non-rate limiting) nucleophilic attack of amines and alcohols to the carbene was observed. The low solubility and poor nucleophilicity of urea explain why nucleophilic attack is rate determining in this case.

2.6 DFT. To further investigate the catalytic mechanism, we pursued DFT calculations to shed light on the nature of the kinetic isotope effect (gas phase, BP86, def2-TZVP, D3). As previous experiments indicated no involvement of the diazo compound in the rate determining step, we first investigated steps A and B to confirm this. As chlorido ligands are known to be displaced from similar ruthenium arene species by carboxamide donors, an intramolecular mechanism in which urea first coordinates to ruthenium (via its carbonyl group) was investigated (Scheme 3b).[35] Coordination of phenyl-2-diazoacetate to the starting complex (Step A, Scheme 3a) was found to be downhill by −2.3 kcal mol^{-1}. Then, release of dinitrogen from the diazo adduct to form the ruthenium carbene was found to have a small barrier of 6 kcal mol^{-1} (Step B, Scheme 3a). This step is strongly exergonic, and release of dinitrogen was found to be downhill by −39.0 kcal mol^{-1}. The barrier $\Delta G^{\ddagger}$ for nucleophilic attack from urea on the carbene (Step C, Scheme 3a) was found to be 11.53 kcal mol^{-1}, in accordance with the experimentally observed fast reaction at room temperature.

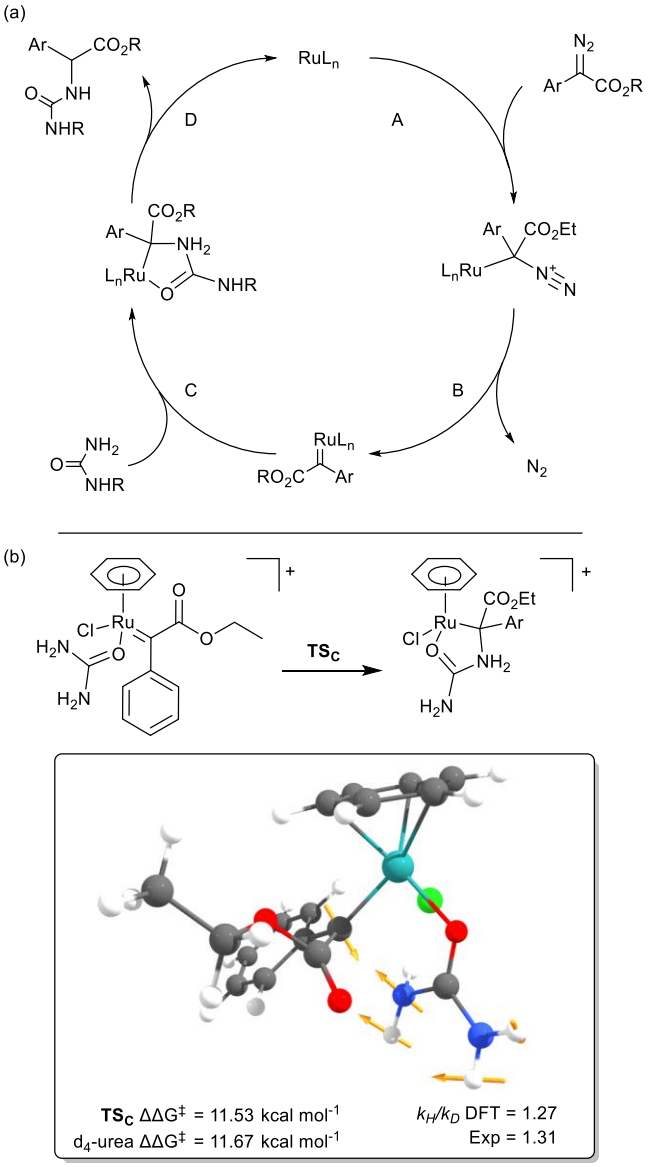

Scheme 3. (a) Catalytic cycle for ruthenium catalyzed carbene N-H insertion. A) Diazo coordination B) Carbene formation C) Nucleophilic attack D) Proton shift. (b) Transition state structure for nucleophilic attack by urea (CPK coloring).

Interestingly, a slight dependence of the transition state energy on the orientation of the was found, if the aryl

moiety is pointing towards the urea the barrier was slightly increased to 12.3 kcal mol^{-1}. By visualizing the displacement vectors a N–H bending vibration can be observed in the intrinsic reaction coordinate of the transition state (Scheme 3b), pointing towards a secondary kinetic isotope effect for deuteration of this position. Furthermore, by recalculating the vibrational correction to the Gibbs free energy of the starting material and the transition state, a DFT estimate of the kinetic isotope effect can be calculated. The transition state barrier for d_4-urea $\Delta\Delta G^{\ddagger}$ was found to be 11.67 kcal mol^{-1} corresponding to k_H/k_D = 1.27, in accordance with the experimentally derived value. The DFT results therefore support nucleophilic attack to be rate determining for the ruthenium-catalyzed copolymerization of urea and bis-diazos. The subsequent proton transfer through a 1,5-proton shift towards the ester moiety was calculated to have a DFT barrier of 13.5 kcal mol^{-1}, however, as this is presumably substrate- or solvent-assisted the experimental barrier in solution is expected to be lower.

2.7 Copolymerization. Commercial polyureas get their unique properties from having a mixture of soft and hard segments within their polymer backbone.[36] This is generally achieved by mixing different polyamines with isocyanates and as such we were interested in whether the developed Ru-catalyzed polycondensation was suitable for copolymerization. To incorporate a soft segment a polytetramethylene oxide (PTMO) oligomer (M_n=1000 g/mol) was end-capped with phenyldiazoacetate units in a two-step procedure.

Table 3. Copolymerization of an end-group functionalized polytetramethyleneoxide (PTMO), diazo 2a and urea.

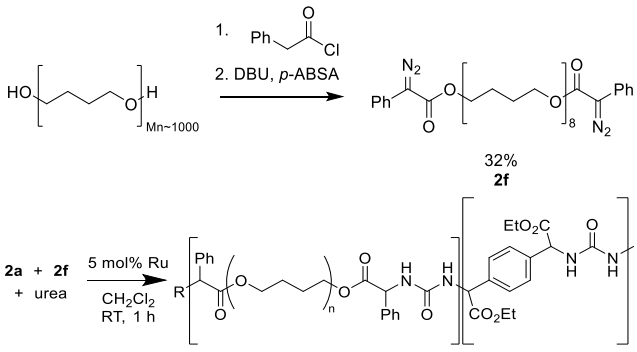

#	2a (mmol)	2f (mmol)	Urea (mmol)	M_w (kDa) [a]	PDI [a]	T_g [b]
3a	100	0	100	4.9	1.54	141
3f	0	100	100	8.3	2.1	34
3g	100	100	200	12.2	2.09	39

Conditions: urea (100 umol), **2b** (100 umol), dichloro(*p*-cymene)ruthenium(II) dimer (2.5 umol), DCM (2.5 mL), room temperature, 1 hour. [a] Determined by SEC in DCM. [b] M_w/M_n as determined by DSC.

First, phenylacetyl chloride was used to introduce phenylacetyl groups after a similar Regitz diazo transfer procedure was used to introduce diazo groups on the end, providing telechelic polymer **2f** (M_n = 1500 g/mol, determined by SEC). When reacted with urea under the optimized polycondensation conditions as described above (Table 3, entry 3f), a polymer with molecular weight of 8.3 kD was obtained indicating successful copolymerization, with a T_g observed at 34 °C (Figure S22). To incorporate more hard blocks within the polymer, copolymerization with diazo **2a** was performed. When telechelic polymer **2f** was copolymerized with **2a**, a material with molecular weight 12.2 kD and a glass transition temperature of 39 °C was obtained. Furthermore, the molecular weight distributions obtained from SEC in all cases displayed monomodal distributions (Figure S22), showing the efficacy to use multiple diazo compounds in copolymerization. Further studies are directed at further tuning the material properties, to not only emulate the molecular structure of polyureas but also to gain the desirable features present in commercial polyureas.

3 Conclusion

In this work, we have demonstrated the capability to synthesize polyureas by ruthenium catalyzed N–H insertion reactions. With this protocol, polyurea moieties are accessible through a route completely free of isocyanate. The formed polymers were found to have material properties tunable through side chain or main chain substitution. The mechanistic investigations show nucleophilic attack of urea on the formed carbene to be rate determining. This work shows the possibility of using diazo compounds in combination with transition metal catalysis to furnish novel routes towards isocyanate-free polyureas.

AUTHOR INFORMATION

Corresponding Author

*Prof. Dr. B. de Bruin. E-mail: b.debruin@uva.nl

Funding Sources

ARC-CBBC 2018.015.C to BdB.

Notes

The authors declare no competing financial interest.

ACKNOWLEDGMENT

Financial support from the Advanced Research Center for Chemical Building Blocks (ARC CBBC, project 2018.015.C and 2019.021.A), which is co-founded and co-financed by the Dutch Research Council (NWO) and the Netherlands Ministry of Economic Affairs and Climate Policy, is gratefully acknowledged. PCML and NY acknowledge the financial support from the Netherlands Organization for Scientific Research (NWO) VIDI program (VI.Vidi.192.045).

References

(1) Howarth, G. Polyurethanes, Polyurethane Dispersions and Polyureas: Past, Present and Future. *Surface Coatings International Part B: Coatings Transactions* **2003**, *86* (2), 111–118. https://doi.org/10.1007/BF02699621.

(2) Yakeya, D.; Yoshida, Y.; Endo, T. Phosgene-Free and Chemoselective Synthesis of Novel Polyureas from Activated l -

Lysine with Diphenyl Carbonate. *Macromolecules* **2020**, *53* (16), 6809–6815. https://doi.org/10.1021/acs.macromol.0c01039.
(3) White, B. T.; Migliore, J. M.; Mapesa, E. U.; Wolfgang, J. D.; Sangoro, J.; Long, T. E. Isocyanate- And Solvent-Free Synthesis of Melt Processible Polyurea Elastomers Derived from Urea as a Monomer. *RSC Advances* **2020**, *10* (32), 18760–18768. https://doi.org/10.1039/d0ra02369h.
(4) Cornille, A.; Auvergne, R.; Figovsky, O.; Boutevin, B.; Caillol, S. A Perspective Approach to Sustainable Routes for Non-Isocyanate Polyurethanes. *European Polymer Journal*. Elsevier Ltd February 1, 2017, pp 535–552. https://doi.org/10.1016/j.eurpolymj.2016.11.027.
(5) Zhou, X.; Li, Y.; Fang, C.; Li, S.; Cheng, Y.; Lei, W.; Meng, X. Recent Advances in Synthesis of Waterborne Polyurethane and Their Application in Water-Based Ink: A Review. *Journal of Materials Science and Technology* **2015**, *31* (7), 708–722. https://doi.org/10.1016/j.jmst.2015.03.002.
(6) Carré, C.; Ecochard, Y.; Caillol, S.; Avérous, L. From the Synthesis of Biobased Cyclic Carbonate to Polyhydroxyurethanes: A Promising Route towards Renewable Non-Isocyanate Polyurethanes. *ChemSusChem*. Wiley-VCH Verlag August 8, 2019, pp 3410–3430. https://doi.org/10.1002/cssc.201900737.
(7) Filippi, L.; Meier, M. A. R. Fully Renewable Non-Isocyanate Polyurethanes via the Lossen Rearrangement. *Macromolecular Rapid Communications* **2021**, *42* (3). https://doi.org/10.1002/marc.202000440.
(8) He, X.; Xu, X.; Wan, Q.; Bo, G.; Yan, Y. Solvent- and Catalyst-Free Synthesis, Hybridization and Characterization of Biobased Nonisocyanate Polyurethane (NIPU). *Polymers (Basel)* **2019**, *11* (6), 1026. https://doi.org/10.3390/polym11061026.
(9) Wu, Z.; Tang, L.; Dai, J.; Qu, J. Synthesis and Properties of Fluorinated Non-Isocyanate Polyurethanes Coatings with Good Hydrophobic and Oleophobic Properties. *Journal of Coatings Technology and Research* **2019**, *16* (5), 1233–1241. https://doi.org/10.1007/s11998-019-00195-5.
(10) Jellema, E.; Jongerius, A. L.; Reek, J. N. H.; de Bruin, B. C1 Polymerisation and Related C-C Bond Forming 'Carbene Insertion' Reactions. *Chemical Society Reviews* **2010**, *39* (5), 1706–1723. https://doi.org/10.1039/b911333a.
(11) Shimomoto, H.; Moriya, T. A.; Mori, T.; Itoh, T.; Kanehashi, S.; Ogino, K.; Ihara, E. Single-Component Polycondensation of Bis(Alkoxycarbonyldiazomethyl)Aromatic Compounds to Afford Poly(Arylene Vinylene)s with an Alkoxycarbonyl Group on Each Vinylene Carbon Atom. *ACS Omega* **2020**, *5* (10), 4787–4797. https://doi.org/10.1021/acsomega.9b03408.
(12) Shimomoto, H.; Itoh, E.; Itoh, T.; Ihara, E.; Hoshikawa, N.; Hasegawa, N. Polymerization of Hydroxy-Containing Diazoacetates: Synthesis of Hydroxy-Containing "Poly(Substituted Methylene)s" by Palladium-Mediated Polymerization and Poly(Ester-Ether)s by Polycondensation through O-H Insertion Reaction. *Macromolecules* **2014**, *47* (13), 4169–4177. https://doi.org/10.1021/ma500783b.
(13) Shimomoto, H.; Mori, T.; Itoh, T.; Ihara, E. Poly(β-Keto Enol Ether) Prepared by Three-Component Polycondensation of Bis(Diazoketone), Bis(1,3-Diketone), and Tetrahydrofuran: Mild Acid-Degradable Polymers to Afford Well-Defined Low Molecular Weight Components. *Macromolecules* **2019**, *52* (15), 5761–5768. https://doi.org/10.1021/acs.macromol.9b00653.
(14) Wang, X.; Ding, Y.; Tao, Y.; Wang, Z.; Wang, Z.; Yan, J. Polycondensation of Bis(α-Diazo-1,3-Dicarbonyl) Compounds with Dicarboxylic Acids: An Efficient Access to Functionalized Alternating Polyesters. *Polymer Chemistry* **2020**, *11* (10), 1708–1712. https://doi.org/10.1039/d0py00185f.
(15) Deng, Q. H.; Xu, H. W.; Yuen, A. W. H.; Xu, Z. J.; Che, C. M. Ruthenium-Catalyzed One-Pot Carbenoid N-H Insertion Reactions and Diastereoselective Synthesis of Prolines. *Organic Letters* **2008**, *10* (8), 1529–1532. https://doi.org/10.1021/ol800087p.
(16) Shimomoto, H.; Mukai, H.; Bekku, H.; Itoh, T.; Ihara, E. Ru-Catalyzed Polycondensation of Dialkyl 1,4-Phenylenebis(Diazoacetate) with Dianiline: Synthesis of Well-Defined Aromatic Polyamines Bearing an Alkoxycarbonyl Group at the Adjacent Carbon of Each Nitrogen in the Main Chain Framework. *Macromolecules* **2017**, *50* (23), 9233–9238. https://doi.org/10.1021/acs.macromol.7b01994.
(17) Chan, W.-W.; Yeung, S.-H.; Zhou, Z.; Chan, A. S. C.; Yu, W.-Y. Ruthenium Catalyzed Directing Group-Free C2-Selective Carbenoid Functionalization of Indoles by α-Aryldiazoesters. *Organic Letters* **2010**, *12* (3), 604–607. https://doi.org/10.1021/ol9028226.
(18) Galardon, E.; le Maux, P.; Simonneaux, G. Insertion of Ethyl Diazoacetate into NH and SH Bonds Catalyzed by Ruthenium Porphyrin Complexes; 1997.
(19) Huang, W. S.; Xu, Z.; Yang, K. F.; Chen, L.; Zheng, Z. J.; Xu, L. W. Modular Construction of Multifunctional Ligands for the Enantioselective Ruthenium-Catalyzed Carbenoid N-H Insertion Reaction:An Enzyme-like and Substrate-Sensitive Catalyst System. *RSC Advances* **2015**, *5* (58), 46455–46463. https://doi.org/10.1039/c5ra05804j.
(20) Padín, D.; Varela, J. A.; Saá, C. Ruthenium-Catalyzed Tandem Carbene/Alkyne Metathesis/N-H Insertion: Synthesis of Benzofused Six-Membered Azaheterocycles. *Organic Letters* **2020**, *22* (7), 2621–2625. https://doi.org/10.1021/acs.orglett.0c00596.
(21) Zhou, Z.; Tan, Y.; Yamahira, T.; Ivlev, S.; Xie, X.; Riedel, R.; Hemming, M.; Kimura, M.; Meggers, E. Enantioselective Ring-Closing C–H Amination of Urea Derivatives. *Chem* **2020**, *6* (8), 2024–2034. https://doi.org/10.1016/j.chempr.2020.05.017.
(22) Fritz, J. A.; Nakhla, J. S.; Wolfe, J. P. A New Synthesis of Imidazolidin-2-Ones via Pd-Catalyzed Carboamination of N-Allylureas. *Organic Letters* **2006**, *8* (12), 2531–2534. https://doi.org/10.1021/ol060707b.
(23) Rao, W. H.; Yin, X. S.; Shi, B. F. Catalyst-Controlled Amino- versus Oxy-Acetoxylation of Urea-Tethered Alkenes: Efficient Synthesis of Cyclic Ureas and Isoureas. *Organic Letters* **2015**, *17* (15), 3758–3761. https://doi.org/10.1021/acs.orglett.5b01741.
(24) Tamaru, Y.; Hojo, M.; Higashimura, H.; Yoshida, Z.; J Am, E. L. Urea as the Most Reactive and Versatile Nitrogen Nucleophile for the Palladium(2+)-Catalyzed Cyclization of Unsaturated Amines Table I. Optimization of Conditions for Aminocarbonylation of A-Benzyl-A-3-Butenyl-A'-Methylurea (Id: R1 = CH2Ph, R2 = Me) Entry Conditions"; Varaprath, S. Ibid, 1988; Vol. 110.
(25) M. L. Davies, H.; v. A. Grazini, M.; Aouad, E. Asymmetric Intramolecular C–H Insertions of Aryldiazoacetates. *Organic Letters* **2001**, *3* (10), 1475–1477. https://doi.org/10.1021/ol0157858.
(26) Green, S. P.; Wheelhouse, K. M.; Payne, A. D.; Hallett, J. P.; Miller, P. W.; Bull, J. A. Thermal Stability and Explosive Hazard Assessment of Diazo Compounds and Diazo Transfer Reagents. *Organic Process Research & Development* **2020**, *24* (1), 67–84. https://doi.org/10.1021/acs.oprd.9b00422.
(27) Tawa, T.; Ito, S. The Role of Hard Segments of Aqueous Polyurethane-Urea Dispersion in Determining the Colloidal Characteristics and Physical Properties. *Polymer Journal* **2006**, *38* (7), 686–693. https://doi.org/10.1295/polymj.PJ2005193.
(28) Reinecker, M.; Soprunyuk, V.; Fally, M.; Sánchez-Ferrer, A.; Schranz, W. Two Glass Transitions of Polyurea Networks: Effect of the Segmental Molecular Weight. *Soft Matter* **2014**, *10* (31), 5729–5738. https://doi.org/10.1039/c4sm00979g.
(29) Slot, T. K.; Shiju, N. R.; Rothenberg, G. A Simple and Efficient Device and Method for Measuring the Kinetics of Gas-Producing Reactions. *Angewandte Chemie* **2019**, *131* (48), 17433–17436. https://doi.org/10.1002/ange.201911005.
(30) Liang, Y.; Zhou, H.; Yu, Z. X. Why Is Copper(I) Complex More Competent than Dirhodium(II) Complex in Catalytic Asymmetric O-H Insertion Reactions? A Computational Study of the

Metal Carbenoid O-H Insertion into Water. *J Am Chem Soc* **2009**, *131* (49), 17783–17785. https://doi.org/10.1021/ja9086566.
(31) Gillingham, D.; Fei, N. Catalytic x–h Insertion Reactions Based on Carbenoids. *Chemical Society Reviews* **2013**, *42* (12), 4918–4931. https://doi.org/10.1039/c3cs35496b.
(32) Bergstrom, B. D.; Nickerson, L. A.; Shaw, J. T.; Souza, L. W. Transition Metal Catalyzed Insertion Reactions with Donor/Donor Carbenes. *Angewandte Chemie - International Edition*. John Wiley and Sons Inc March 22, 2021, pp 6864–6878. https://doi.org/10.1002/anie.202007001.
(33) Anslyn, E. v.; Dougherty, D. A. *Modern Physical Organic Chemistry*; University Science Books: Sausalito, California, 2006.
(34) Bacchi, A.; Pelagatti, P.; Pelizzi, C.; Rogolino, D. Diastereomeric Half-Sandwich Ru(II) Cationic Complexes Containing Amino Amide Ligands. Synthesis, Solution Properties, Crystal Structure and Catalytic Activity in Transfer Hydrogenation of Acetophenone. *Journal of Organometallic Chemistry* **2009**, *694* (19), 3200–3211. https://doi.org/10.1016/j.jorganchem.2009.05.010.
(35) Chen, Z. S.; Yang, W. P.; Macosko, C. W. Polyurea Synthesis and Properties as a Function of Hard-Segment Content. *Rubber Chemistry and Technology* **1988**, *61* (1), 86–99. https://doi.org/10.5254/1.3536179.

Entry for the Table of Contents